Frontiers in Built Environment

TYPE Original Research
PUBLISHED 16 May 2023
DOI 10.3389/fbuil.2023.1129175

Check for updates

OPEN ACCESS

EDITED BY
Xinzheng Lu,
Tsinghua University, China

REVIEWED BY
Ercan Işık,
Bitlis Eren University, Türkiye
Francesco Clementi,
Marche Polytechnic University, Italy

*CORRESPONDENCE
Francesca Linda Perelli,
francescalinda.perelli@unina.it

RECEIVED 21 December 2022
ACCEPTED 27 April 2023
PUBLISHED 16 May 2023

CITATION
Perelli FL, Di Maio LS, De Gregorio D, Magliulo G, De Martino P and Zuccaro G (2023), Impact assessment caused by bradyseism phenomena in the Campi Flegrei area.
Front. Built Environ. 9:1129175.
doi: 10.3389/fbuil.2023.1129175

Impact assessment caused by bradyseism phenomena in the Campi Flegrei area

Francesca Linda Perelli[1]*, Luigia Sara Di Maio[2], Daniela De Gregorio[1,3], Gennaro Magliulo[3], Prospero De Martino[4] and Giulio Zuccaro[1,3]

[1]PLINIVS Study Centre, University of Naples Federico II, Naples, Italy, [2]Department of Earth Sciences, University of Geneva, Geneva, Switzerland, [3]Department of Structures for Engineering and Architecture (DiSt), University of Naples Federico II, Naples, Italy, [4]Istituto Nazionale di Geofisica e Vulcanologia, Sez. di Napoli–Osservatorio Vesuviano, Naples, Italy

Campi Flegrei (Italy) is among the areas with the greatest volcanic explosive risk in the world due to the dangerousness of the expected hazards, the high exposed value (about 500,000 people will be evacuated during the “alarm phase”), and the vulnerability of the urban settlements under the effect of the volcanic phenomena. The last two dramatic bradyseism phases occurred in 1969–1972 and 1982–1984 when Pozzuoli town was affected by rapid ground inflation, which brought an overall higher level of about 3.5 m and caused numerous earthquakes ($M \leq 4.2$), with severe damage to buildings. During 1984, the seismicity was intense, with 33 events with $0.5 < M \leq 3$ and six with $3 < M \leq 3.8$. Subsequently, the Campi Flegrei caldera was characterized by general subsidence for about 20 years until 2005, when a new inflation period started and is still ongoing (~1 m). The areal distribution of the recent uplift is characterized by the maximum vertical displacement in the town of Pozzuoli, with a radial decrease from the caldera center outwards. The need to better understand Campi Flegrei volcanic activity is fundamental to protecting the population from hazards linked to explosive volcanic eruptions and understanding the role of seismicity as a possible precursor of a potential eruption. In this perspective, as part of the activities of the PLINIVS Study Centre (Centre of Competence of Italian Civil Protection Department for Volcanic Risk), the authors developed a procedure, implemented in a web application, that relates the monitoring of the ground deformation with the behavior of buildings to evaluate the level of progressive damage to the ordinary Phlegraean buildings due to bradyseism in near real time. This study describes the models adopted for the three impact/risk factors (hazard, exposure, and vulnerability) used to estimate building damage.

KEYWORDS

bradyseism, fragility curves, volcanic risk, building safety check, emergency plan

1 Introduction

Campi Flegrei is a large and potentially very explosive volcanic area (Jenkins et al., 2015; Marzocchi et al., 2015; Aucelli et al., 2017; Vitale et al., 2019; Cannatelli et al., 2020) made by a caldera collapse structure (Orsi et al., 1996; Di Vito et al., 1999; Deino et al., 2004), with the concrete possibility of high-impact eruptions (Horwell et al., 2015). It is characterized by a volcanic phenomenon called “bradyseism” (from the Greek *bradus*, which means slow, and *sism*, which means movement), which is a short-term ground deformation (Orsi et al., 1999) determining a slow ground uplift and subsidence according to a bell-shaped geometry. The derived deformation is made by vertical and horizontal displacements. Earthquakes manifest themselves mainly as seismic swarms, always following the deformation produced by the uplift (Tramelli et al., 2006; Giudicepietro et al., 2021; Lima et al., 2021). The Campi Flegrei area suffered two bradyseismic crises in recent times, the first between 1969 and 1972, the second between 1982 and 1984, with critical seismic activity and abnormal ground inflation, reaching a total uplift of 3.56 m (177 cm during the first crisis, 179 during the second) (Del Gaudio et al., 2010).

The knowledge of the bradyseismic phenomenon in the Campi Flegrei area and its impact on the built stock is important for the (very dense) population safety. Extensive literature deals with the analytic study of the effects of soil motion on building behavior, especially for masonry structures, from a kinematic (Iannuzzo et al., 2018; Iannuzzo et al., 2021; Liguori et al., 2022; Maia Avelino et al., 2022; Perelli et al., 2023a) and static (Cusano et al., 2021; Montanino et al., 2022) standpoint.

The PLINIVS Study Centre developed for the Italian Civil Protection is a procedure that relates the monitoring of soil motion to building behavior to evaluate the level of ordinary Phlegraean building progressive damage due to bradyseism in near real time. The tool has been automated in a web application available at the Civil Protection Department, which returns, for each square area with a side of 250 m (minimum unit of analysis), the number of buildings with an assigned damage level (from D0, no damage, to D5, total collapse), depending on soil slope and uplift inputs. Some similar web applications can be found in the literature with respect to seismic events (Işık et al., 2018; Işık et al., 2021; Columbro et al., 2022; Nanda et al., 2022; Zhang et al., 2022).

The procedure provides scenario analyses based on hazard, exposure, and vulnerability. The hazard is provided in terms of slope and uplift through a periodic automatic transfer in the web application, where two different monitored pieces of information are acquired: the CNR-IREA interferometric data and the INGV-OV geodetic network data. The exposure is assessed through the distribution on the territory of the typological–structural characteristics of the buildings. It is estimated by statistical procedures based on information obtained through detailed data collection campaigns on the territory, including about 2,000 buildings in Pozzuoli town, and data on buildings provided by the National Census Building Database (ISTAT, 2001). The vulnerability of the building stock is developed on an empirical basis from the analysis of the damage to the Puteolan building stock following the 1982–1984 bradyseismic crisis, recorded in special survey forms called POZZUOLI, provided by the Municipality of Pozzuoli, integrated by Perelli et al. (2019) for the not surveyed buildings. Fragility curves have been assessed depending on soil slope and uplift for three bradyseismic vulnerability classes (A, B, and C for decreasing vulnerability), in which the buildings are grouped according to their typological–structural characteristics. Based on the SAVE method (Zuccaro and Cacace, 2015), an empirical model has been constructed using data collected by the POZZUOLI form capable of assigning a bradyseismic fragility class to a building based on its typological characteristics (bradyseismic SAVE). According to the BINC procedure (Cacace et al., 2018), statistical correlations were determined between bradyseismic fragility classes and the year of building construction. A possible distribution of building fragility over the analyzed territory was determined using the ISTAT 2011 database (ISTAT, 2001), which provides the number of buildings by the age of construction over census areas.

2 The event of 1982–1984: building damage dataset

2.1 Building safety check: POZZUOLI form

During the bradyseismic crisis in 1982–1984, the Secretary of State Minister for Coordination of Civil Protection promoted and coordinated a census of the constructions aimed at deepening the knowledge of the static conditions of the buildings in Pozzuoli and assessing a structural safety check for each of them. For this purpose, an *ad hoc* form, called the POZZUOLI form, was developed (Figures 1, 2) by a Technical Scientific Committee (TSC) on the basis of the form tested for the 1980 Irpinia earthquake.

The form defines the state of the construction and collects data useful to the structural safety judgment. The data are grouped into two pages of the form (Figures 1, 2), and they are divided into ten sections: date, building location, metric data, intended use, structural characteristics, previous interventions, damage, vulnerability, structural suitability, and comments.

Page 1 of the POZZUOLI form (Figure 1) comprises six sections. Section 1 contains information on the date of the survey activity, the team identifier, and the order number of the structural unit under examination (isolated or in structural aggregate). Section 2 collects data on the location (address) and context (old town, urban area, and rural area) of the building. Section 3 collects metric data of the building, such as surface, height, volume, number of floors above ground level, number of underground floors, presence of attic, and the possible presence of fronts common to other buildings. Section 4 relates to the intended use of the building (residential or productive) and the possible annexed structures. Section 5 collects the structural characteristics of the building, including age and construction techniques for vertical and horizontal structures and the roof. Section 6 contains information on possible previous structural interventions.

Page 2 of the POZZUOLI form (Figure 2) comprises four sections. Section 7 contains an assessment of damage on vertical structures, floors, roofs, external infill panels, partitions, and stairs, according to eight levels of judgment: no damage, irrelevant, slight, notable, severe, very severe, partially collapsed, and collapsed. Section 8 presents information on vulnerability factors, divided by masonry and reinforced concrete typologies and the assessment of a vulnerability index. Section 9 presents the structural safety check of the building through suitability expert judgment. Section 10 contains a note space for observations.

A total of 3,695 buildings were examined using the POZZUOLI form (Figure 3), including 2,726 masonry buildings and 969 reinforced concrete buildings. The aggregates were 361, and the interconnected (in aggregates) structural units were 1,144 globally.

10.3389/fbuil.2023.1129175

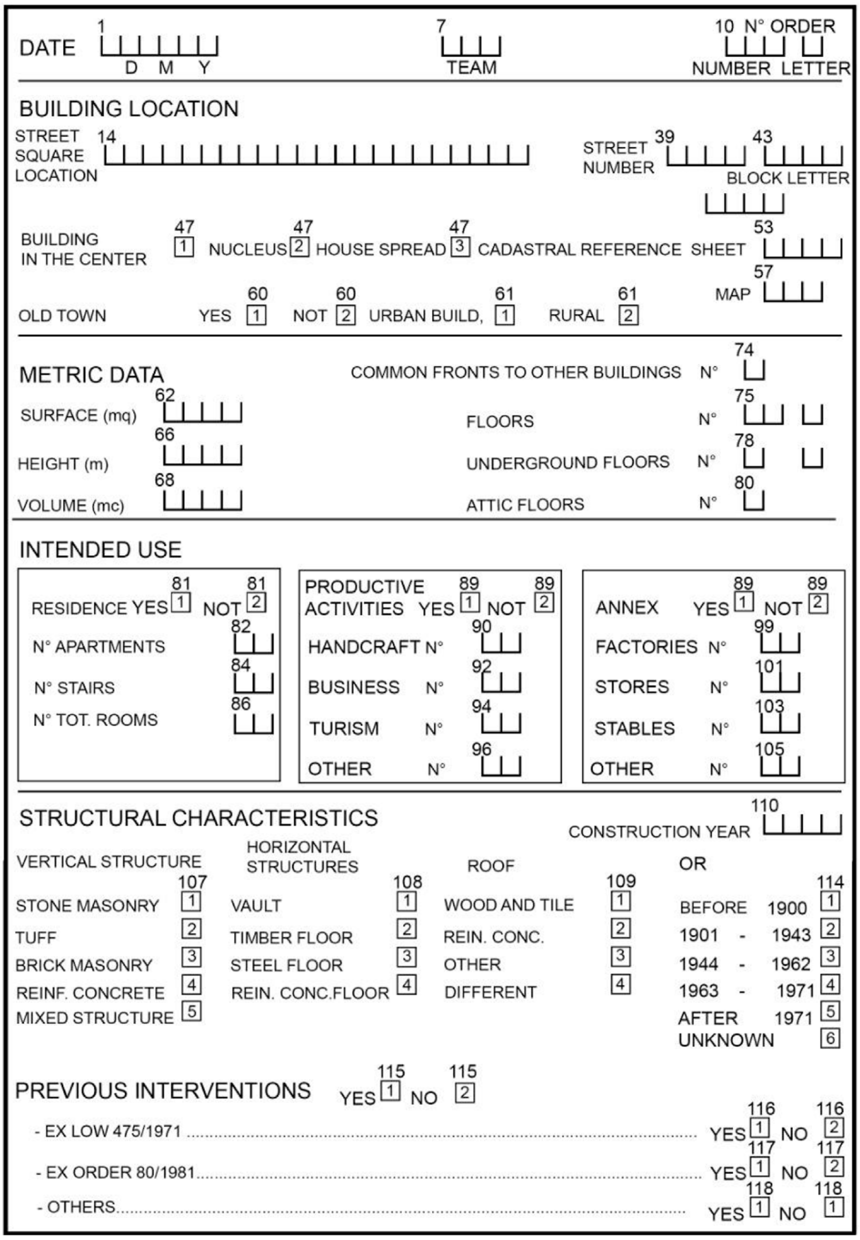
DATE 1 D M Y
7 TEAM
10 N° ORDER NUMBER LETTER

BUILDING LOCATION
STREET SQUARE LOCATION 14
STREET NUMBER 39
43 BLOCK LETTER
BUILDING IN THE CENTER 47 [1] NUCLEUS 47 [2] HOUSE SPREAD 47 [3] CADASTRAL REFERENCE SHEET 53
57 MAP
OLD TOWN YES 60 [1] NOT 60 [2] URBAN BUILD. 61 [1] RURAL 61 [2]

METRIC DATA
COMMON FRONTS TO OTHER BUILDINGS N° 74
SURFACE (mq) 62
FLOORS N° 75
HEIGHT (m) 66
UNDERGROUND FLOORS N° 78
VOLUME (mc) 68
ATTIC FLOORS N° 80

INTENDED USE
RESIDENCE YES 81 [1] NOT 81 [2]
N° APARTMENTS 82
N° STAIRS 84
N° TOT. ROOMS 86
PRODUCTIVE ACTIVITIES YES 89 [1] NOT 89 [2]
HANDCRAFT N° 90
BUSINESS N° 92
TURISM N° 94
OTHER N° 96
ANNEX YES 89 [1] NOT 89 [2]
FACTORIES N° 99
STORES N° 101
STABLES N° 103
OTHER N° 105

STRUCTURAL CHARACTERISTICS
CONSTRUCTION YEAR 110
VERTICAL STRUCTURE 107: STONE MASONRY [1], TUFF [2], BRICK MASONRY [3], REINF. CONCRETE [4], MIXED STRUCTURE [5]
HORIZONTAL STRUCTURES 108: VAULT [1], TIMBER FLOOR [2], STEEL FLOOR [3], REIN. CONC.FLOOR [4]
ROOF 109: WOOD AND TILE [1], REIN. CONC. [2], OTHER [3], DIFFERENT [4]
OR 114: BEFORE 1900 [1], 1901 - 1943 [2], 1944 - 1962 [3], 1963 - 1971 [4], AFTER 1971 [5], UNKNOWN [6]

PREVIOUS INTERVENTIONS YES 115 [1] NO 115 [2]
- EX LOW 475/1971 .... YES 116 [1] NO 116 [2]
- EX ORDER 80/1981 .... YES 117 [1] NO 117 [2]
- OTHERS .... YES 118 [1] NO 118 [1]

FIGURE 1
Pozzuoli form, page 1.

2.2 Analyses of correlations between the building characteristics and the damage

Based on the SAVE approach (Zuccaro and Cacace, 2015) developed in the seismic field, the data collected following the 1982–1984 events have been analyzed to calibrate a statistical procedure that can understand the behavior of buildings in the case of bradyseism phenomena. In particular, the correlations between data on building features and damage have been determined.

For each building, there are four typological–structural characteristics deduced using the POZZUOLI form: the vertical typology (stone masonry, tuff, brick masonry, reinforced concrete, and mixed structure); the horizontal typology (vault, timber floor, steel floor, and reinforced concrete); the number of floors (1–12, but grouped in 1–2, 3–4, 5–6, and 7+); and the age of the construction (before 1900, 1901–1943, 1944–1962, 1963–1971, and after 1971). The type of roof is not considered because the information is not always clearly defined for the available sample.

The damage collected in the POZZUOLI form is expressed on a scale of eight levels. In this work, damage information has been defined according to the European Macroseismic Scale-98 (Grünthal, 1998) scale, which is structured on six grades representing the overall damage of the structure: D5, total collapse; D4, partial collapse; D3, severe structural damage; D2, light structural damage; D1, light nonstructural damage; and D0, no

10.3389/fbuil.2023.1129175

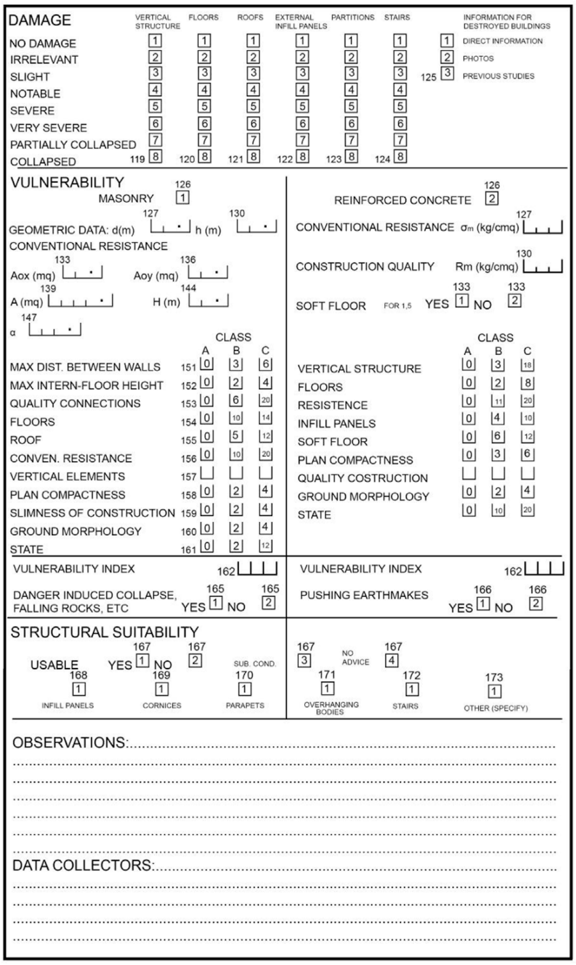
DAMAGE

	VERTICAL STRUCTURE	FLOORS	ROOFS	EXTERNAL INFILL PANELS	PARTITIONS	STAIRS
NO DAMAGE	1	1	1	1	1	1
IRRELEVANT	2	2	2	2	2	2
SLIGHT	3	3	3	3	3	3
NOTABLE	4	4	4	4	4	4
SEVERE	5	5	5	5	5	5
VERY SEVERE	6	6	6	6	6	6
PARTIALLY COLLAPSED	7	7	7	7	7	7
COLLAPSED	119 8	120 8	121 8	122 8	123 8	124 8

INFORMATION FOR DESTROYED BUILDINGS: 1 DIRECT INFORMATION; 2 PHOTOS; 125 3 PREVIOUS STUDIES

VULNERABILITY

MASONRY 126 1 — REINFORCED CONCRETE 126 2

GEOMETRIC DATA: d(m) 127 h (m) 130 — CONVENTIONAL RESISTANCE σm (kg/cmq) 127

CONVENTIONAL RESISTANCE — CONSTRUCTION QUALITY Rm (kg/cmq) 130

Aox (mq) 133 Aoy (mq) 136

A (mq) 139 H (m) 144 — SOFT FLOOR FOR 1,5 YES 133 1 NO 133 2

α 147

CLASS	A	B	C
MAX DIST. BETWEEN WALLS	151 0	3	6
MAX INTERN-FLOOR HEIGHT	152 0	2	4
QUALITY CONNECTIONS	153 0	6	20
FLOORS	154 0	10	14
ROOF	155 0	5	12
CONVEN. RESISTANCE	156 0	10	20
VERTICAL ELEMENTS	157		
PLAN COMPACTNESS	158 0	2	4
SLIMNESS OF CONSTRUCTION	159 0	2	4
GROUND MORPHOLOGY	160 0	2	4
STATE	161 0	2	12

CLASS	A	B	C
VERTICAL STRUCTURE	0	3	18
FLOORS	0	2	8
RESISTENCE	0	11	20
INFILL PANELS	0	4	10
SOFT FLOOR	0	6	12
PLAN COMPACTNESS	0	3	6
QUALITY COSTRUCTION			
GROUND MORPHOLOGY	0	2	4
STATE	0	10	20

VULNERABILITY INDEX 162 — VULNERABILITY INDEX 162

DANGER INDUCED COLLAPSE, FALLING ROCKS, ETC YES 165 1 NO 165 2 — PUSHING EARTHMAKES YES 166 1 NO 166 2

STRUCTURAL SUITABILITY

USABLE YES 167 1 NO 167 2 — 167 3 NO ADVICE 167 4

168 1 INFILL PANELS; 169 1 CORNICES; SUB. COND. 170 1 PARAPETS; 171 1 OVERHANGING BODIES; 172 1 STAIRS; 173 1 OTHER (SPECIFY)

OBSERVATIONS:

DATA COLLECTORS:

FIGURE 2
Pozzuoli form, page 2.

damage. The correlation between the two damage scales was set based on the damage indicated on the vertical structure, horizontal structures, and interior infill panels of the POZZUOLI form because these are the most filled data in the database. The correspondence has been set as follows: D5: the damage of the vertical and horizontal structures is marked as "collapsed"; D4: at least one damage scale of the vertical structure or that of the horizontal structures is marked as "partially collapsed" or "very severe" and the other is marked as other than "collapsed"; D3: at least one damage scale of the vertical structure and that of the horizontal structures is marked as "severe" or "notable," and the other is other than "collapsed" or "partially collapsed"; D2: at least one between the damage of the vertical structure and that of the horizontal structure is marked as "slight," and the other is other than "collapsed," "partially collapsed," "very severe," "severe," or "notable"; D1: at least one between the damage of the vertical structure and the damage of the horizontal structures is marked as "irrelevant" or both the damage of the vertical structure and the damage of the horizontal structures are crossed out as "no damage" and the damage of the interior infill panels is other than "no damage"; and D0: damage of vertical and horizontal structures and interior infill panels is marked as "no damage."

According to the SAVE approach, on the basis of the correlations among typological–structural characteristics of the building and occurred damage, it is possible to assess a parameter that allows to identify buildings with similar behaviors (similar damage) in regard to the bradyseismic phenomenon and group them into specific classes (called "vulnerability classes"). Accordingly, it is necessary to calculate the barycentric abscissa of the damage level i, called the Synthetic Parameter of Damage (SPD_{Pj}) relative to each category j (described in the following) of each typological feature P (vertical structure, horizontal structure, number of floors, and age), through the relation (Eq. 1). Table 1 summarizes the obtained results.

In particular,

$$\mathrm{SPD}_{P_j} = \frac{\sum_{i=0}^{5} i \cdot \mathrm{N}_{P_{ji}}}{\mathrm{N}_{P_j}} \tag{1}$$

where SPD_{Pj} is the Synthetic Parameter of Damage relative category j of feature P, included in the range [0, 5]; i is the level of damage (0, 1, 2, 3, 4, and 5); P is the building feature (V, vertical structure; H, horizontal structure; F, number of floors; and A, age); j is the category of each feature P (e.g., in the case of vertical structure, j is stone masonry, tuff, brick masonry, reinforced concrete, mixed structure); $\mathrm{N}_{P_{ji}}$ is the number of buildings with feature P of category j and level of damage i; and N_{P_j} is the number of buildings with feature P of category j.

By assuming the "vertical structure" V as a reference parameter, the relative influence of the other features P (horizontal structure, number of floors, and age of construction) on it is calculated as follows:

$$\Delta_{V_j P_k} = \mathrm{SPD}_{P_k} - \mathrm{SPD}_{V_j}, \tag{2}$$

where $\Delta_{V_j P_k}$ is the relative influence parameter of category k of feature P on the category j of the vertical structure feature V; SPD_{V_j} is the Synthetic Parameter of Damage relative to the category j of the vertical structure feature V; and SPD_{P_k} is the Synthetic Parameter of Damage relative to category k of feature P (horizontal structure, number of floors, and age of construction) assessed on a smaller sample of buildings with category j of feature V.

Tables 2, 3, 4 summarize the scores calculated with reference to the parameters' horizontal structure, number of floors, and age, respectively. For each building, it is possible to evaluate a synthetic damage parameter that considers the contribution of vertical structure damage and the relative influence of the other features as follows:

$$SPD = \mathrm{SPD}_{\mathrm{V_j}} + \frac{\sum_P \Delta_{\mathrm{V_j P_k}} \cdot \sum_Q c_{P_k Q_l}}{2\,(m-1)} \tag{3}$$

where SPD is the Synthetic Parameter of Damage to the building, included in the range [0, 5]; $c_{P_k Q_l}$ is the non-correlation coefficient between categories k and l of features P and Q, respectively, assessed by relation (Eq. 4); and m is the number of correlated parameters for the building (≤ 3):

$$c_{P_k Q_l} = 1 - \frac{N_{P_k Q_l}}{N_{P_k}} \tag{4}$$

where $N_{P_k Q_l}$ is the number of buildings with category k for feature P and category l for feature Q and N_{P_k} is the number of

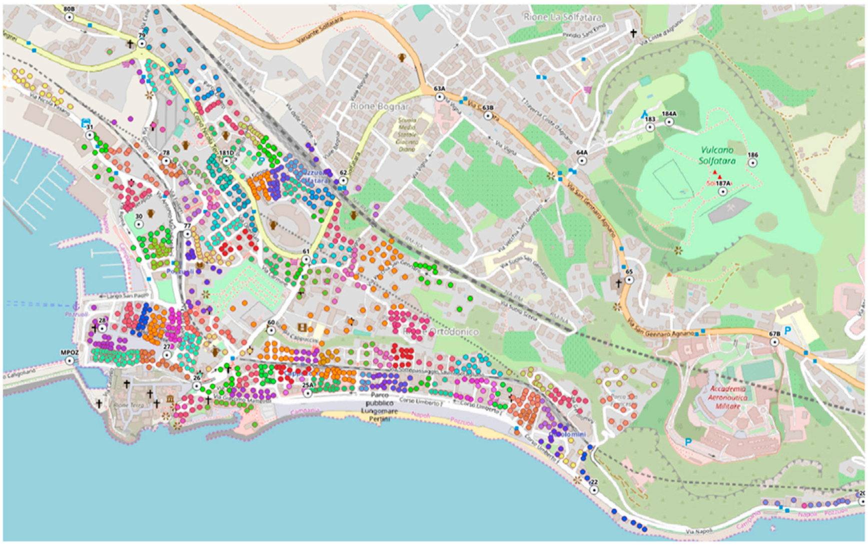

FIGURE 3
Map of the buildings surveyed using the Pozzuoli form.

TABLE 1 Synthetic Parameter of Damage (SPD) for each category of the typological–structural characteristics.

Vertical structure	SPD_V	Buildings (n°)	Horizontal structure	SPD_H	Buildings (n°)
Reinforced concrete	1.29	791	R.C. floor	1.63	1,709
Brick masonry	1.85	26	Steel floor	2.53	898
Stone masonry	2.87	45	Timber floor	3.30	252
Tuff	2.47	1,841	Vault	3.09	128
Mixed structure	1.91	321			
Age of construction	**SPD_H**	**Buildings (n°)**	**Floors**	**SPD_F**	**Buildings (n°)**
Before 1900	3.08	301	1–2	2.07	1,547
1901–1943	2.73	407	3–4	2.18	1,312
1944–1962	2.03	777	5–6	1.94	171
1963–1971	1.60	697	7+	1.38	13
After 1971	1.33	475			

buildings with category k for feature P. The non-correlation coefficients calculated by the POZZUOLI form on the sample of buildings are summarized in Table 5.

Buildings can be classified according to three vulnerability classes (A, B, and C) based on the following SPD ranges, computed assuming the vertical structures SPD (Table 1) as a reference: SPD $\geq$ 2.47 Class A, 1.87 $\leq$ SPD $<$ 2.47 Class B, and SPD $<$ 1.87 Class C.

2.3 Empirical fragility curves

Fragility curves represent the probability that a fixed level of damage can be achieved or exceeded. The vulnerability curves can be estimated through analytical, empirical, or hybrid methods (Calvi et al., 2006). The first one studies building vulnerability through mechanical analyses that can describe the damage evolution of a building with the assigned typological and structural characteristics, increasing the hazard input value. The second one defines building behavior by exploiting detected data about structures affected by seismic events since statistical correlation and regression methods to evaluate the relation among typological characteristics of the buildings, hazard input, and level of damage. The third one combines mechanical and observational analyses of the damage produced by past events. Some recent works (Harrichian, 2021; Nanda et al., 2022) also exploited rapid visual screening through soft computing techniques to define the vulnerability class of the buildings.

TABLE 2 Influence of the horizontal structures on the vertical typologies.

Vertical structure	Horizontal structure	Buildings (n°)	SPD_V	SPD_H	$\Delta_{V_j H_k}$
Reinforced concrete	R.C. floor	780	1.29	1.29	0.00
Reinforced concrete	Steel floor	—	1.29	—	—
Reinforced concrete	Timber floor	—	1.29	—	—
Reinforced concrete	Vault	—	1.29	—	—
Brick masonry	R.C. floor	8	1.85	1.75	−0.10
Brick masonry	Steel floor	16	1.85	1.81	−0.03
Brick masonry	Timber floor	2	1.85	2.50	0.65
Brick masonry	Vault	—	1.85	0.00	−1.85
Stone masonry	R.C. floor	—	2.87	—	—
Stone masonry	Steel floor	17	2.87	2.53	−0.34
Stone masonry	Timber floor	17	2.87	3.18	0.31
Stone masonry	Vault	8	2.87	3.00	0.13
Tuff	R.C. floor	657	2.47	1.96	−0.51
Tuff	Steel floor	811	2.47	2.56	0.08
Tuff	Timber floor	230	2.47	3.34	0.86
Tuff	Vault	117	2.47	3.11	0.63
Mixed structure	R.C. floor	264	1.91	1.81	−0.10
Mixed structure	Steel floor	46	1.91	2.39	0.48
Mixed structure	Timber floor	2	1.91	2.00	0.09
Mixed structure	Vault	3	1.91	2.67	0.76

In this work, empirical fragility curves of ordinary buildings are proposed based on the damage that occurred during the 1982–1984 crisis. The movements that occurred in the 1982–1984 crisis have been studied to analyze the correlation among the vulnerability classes (i.e., the structural–typological features of the buildings), the reached damage, and the bradyseism hazard. The data were furnished by the INGV geodetic network recording the vertical ground movements related to the strongholds distributed throughout the Campi Flegrei territory (Del Gaudio et al., 2010). Bradyseism is a phenomenon that consists of a periodic lowering or raising of the ground level. The hazard caused by the phenomenon can, therefore, be identified in the average variation in height that concerns an area (uplift) or in the lifting differences created between the structural elements of the buildings (slope). In order to evaluate a correlation between the damage to the buildings and the uplift caused by bradyseism, the maximum vertical movements (m) that occurred up to June 1984 were deduced from the provided geodetic data. A continuous distribution of the phenomenon has been evaluated through interpolation by the b-spline function (Figure 4). This enabled the evaluation of the uplift and slope relative to the center of gravity of each building plan surveyed using the POZZUOLI form.

The correlation between the vulnerability classes, damage, and hazard parameters (uplift and slope) provided by INGV has been determined. The results related to total buildings are shown in Table 6. They show a clear underestimation of the damage level D0. Experience testifies that vulnerability models built on an observational basis are often affected by an underestimation of low damage levels caused by the failure to survey undamaged buildings, although affected by the studied phenomenon (Perelli et al., 2019). A confirmation of the lack of such data is shown in Figure 5, which depicts both the strongholds of the INGV stations, where the uplift data related to the 1982–1984 bradyseismic event are recorded, and the buildings surveyed using the POZZUOLI form. In particular, the strongholds are represented by two concentric circles whose red intensity increases as the uplift increases, whereas the damaged buildings are represented by squares whose orange intensity increases as their level of damage increases. Therefore, it is evident that the survey activity mainly focused on the most damaged buildings, also distributed around the strongholds that reached the greatest displacements.

For an accurate definition of the vulnerability model, it is necessary to define a criterion for the recovery of missing data to create a tool able to describe the complete damage evolution of building types for each considered hazard phase. This requires integrating undamaged buildings of the 1982–1984 stock, distributed by vulnerability class and hazard level of the 1982–1984 event. Therefore, the procedure described in

TABLE 3 Influence of the number of floors on the vertical typologies.

Vertical structure	Number of floors	Buildings (n°)	SPD_V	SPD_F	$\Delta_{V_j F_k}$
Reinforced concrete	1–2	272	1.29	1.20	−0.09
Reinforced concrete	3–4	412	1.29	1.31	0.02
Reinforced concrete	5–6	90	1.29	1.48	0.19
Reinforced concrete	7+	11	1.29	1.27	−0.02
Brick masonry	1–2	19	1.85	1.84	0.00
Brick masonry	3–4	5	1.85	2.00	0.15
Brick masonry	5–6	2	1.85	1.50	−0.35
Brick masonry	7+	—	1.85	—	—
Stone masonry	1–2	38	2.87	2.84	−0.02
Stone masonry	3–4	7	2.87	3.00	0.13
Stone masonry	5–6	—	2.87	—	—
Stone masonry	7+	—	2.87	—	—
Tuff	1–2	1,028	2.47	2.33	−0.14
Tuff	3–4	742	2.47	2.66	0.19
Tuff	5–6	58	2.47	2.57	0.10
Tuff	7+	1	2.47	1.00	−1.47
Mixed structure	1–2	179	1.91	1.75	−0.16
Mixed structure	3–4	120	1.91	2.11	0.20
Mixed structure	5–6	19	1.91	2.21	0.30
Mixed structure	7+	1	1.91	3.00	1.09

Section 2.2, based on census data on buildings constructed before 1980, has been adopted.

Summing the number of buildings grouped for vulnerability class and hazard value, the total number of buildings associated with each of these values is obtained (Table 7). The number of undamaged buildings has been determined (D0 value in Table 8) by subtracting the number of damaged buildings from the total number of buildings for each vulnerability class and each hazard value. The pair of logarithmic mean and logarithmic standard deviation parameters that best fit the trend of representative points of cumulative damage rates for each class and each hazard parameter have been evaluated using the least squares method (Figure 6 for slope and Figure 7 for uplift).

3 Impact model

3.1 Scenario analyses

A procedure based on scenario analysis has been developed to evaluate in near real time the damage induced to buildings by uplifts or slopes caused by the bradyseismic phenomenon in the Phlegraean area based on previous studies on seismic impact analyses (Zuccaro et al., 2021a; Zuccaro et al., 2021b; Perelli et al., 2023b). The scenario to achieve an assigned damage level "l" under the effect of an assigned uplift (or slope) is determined as follows:

$$scenario_{l,i} = \int_m q_m \left[(H_i) \cdot (V_{l,i,m}) \right] \tag{5}$$

where H_i is the intensity value of the bradyseismic hazard (uplift or slope) registered by networks in the Campi Flegrei area; $V_{l,i,m}$ is the vulnerability, which is the probability of achieving an assigned damage level "l" by a specific category "m" (vulnerability class) of elements; and q_m characterizes the exposure as the percentage of exposed elements of category "m."

The procedure, implemented in a specific web application, connects three centers of competence of Civil Protection (PLINIVS, INGV-OV, and CNR-IREA) to correlate the records of the movements induced by the bradyseismic phenomenon of the geodetic and interferometric networks with exposure and vulnerability models for evaluating the induced damage. The minimum unit of analysis of the model is a square cell with a side of 250 m. The individual parameters of the model are described in the following sections.

3.2 Hazard

The hazard model provides each minimum unit of analysis (250 × 250 m) the parameters against which the bradyseismic

TABLE 4 Influence of the age of construction on the vertical typologies.

Vertical structure	Age of construction	Buildings (n°)	SPD_V	SPD_A	$\Delta_{V_j A_k}$
Reinforced concrete	Before 1900	—	1.29	—	—
Reinforced concrete	1901–1943	1	1.29	3.00	1.71
Reinforced concrete	1944–1962	129	1.29	1.46	0.17
Reinforced concrete	1963–1971	379	1.29	1.32	0.03
Reinforced concrete	After 1971	262	1.29	1.16	−0.13
Brick masonry	Before 1900	1	1.85	2.00	0.15
Brick masonry	1901–1943	2	1.85	2.00	0.15
Brick masonry	1944–1962	5	1.85	2.40	0.55
Brick masonry	1963–1971	4	1.85	1.25	−0.60
Brick masonry	After 1971	8	1.85	1.63	−0.22
Stone masonry	Before 1900	29	2.87	3.10	0.24
Stone masonry	1901–1943	7	2.87	2.71	−0.15
Stone masonry	1944–1962	1	2.87	2.00	−0.87
Stone masonry	1963–1971	1	2.87	2.00	−0.87
Stone masonry	After 1971	2	2.87	2.50	−0.37
Tuff	Before 1900	258	2.47	3.13	0.65
Tuff	1901–1943	385	2.47	2.74	0.27
Tuff	1944–1962	521	2.47	2.17	−0.30
Tuff	1963–1971	212	2.47	2.00	−0.48
Tuff	After 1971	151	2.47	1.51	−0.96
Mixed structure	Before 1900	11	1.91	2.27	0.36
Mixed structure	1901–1943	12	1.91	2.58	0.67
Mixed structure	1944–1962	121	1.91	1.98	0.07
Mixed structure	1963–1971	100	1.91	1.84	−0.07
Mixed structure	after 1971	52	1.91	1.60	−0.31

behavior of buildings is defined: slope, measured in degrees, and uplift, measured in meters.

The modalities of hazard data acquisition agree with CNR IREA and INGV-OV that provided periodic uploads of Campi Flegrei ground deformation data to the PLINIVS server in the framework of an agreement involving the analysis (monitoring and data processing) of the entire Campi Flegrei area. Accounts have been configured on the server to accept the upload via SFTP of the data surveys, with the expected cadence (monthly/weekly), and credentials for access shared with the institutes' managers.

The provisions and reliabilities of ground deformation data provided by CNR-IREA and INGV-OV are significantly different: CNR-IREA data are recorded by radar interferometry on a 30 × 30-m grid of points covering the entire Campi Flegrei area; INGV-OV provides east, north, and vertical components of Global Navigation Satellite System (GNSS) displacements at 21 Global Positioning System (GPS) stations (De Martino et al., 2021). Therefore, the hazard model has been built upon the CNR-IREA data, and INGV-OV data have been used to validate elaborations. The results of CNR-IREA's satellite Synthetic Aperture Radar (SAR) surveys are provided in a file in which information is organized in an ASCII text table. Each table row provides the following parameters: point identifier, latitude, longitude, strain rate, and uplift. The results are represented on the Shuttle Radar Topography Mission (SRTM) 1 arcsec Digital Elevation Model (DEM) grid. Consequently, the geolocation accuracy corresponds to ± 30 m, and the latitude and longitude provided are relative to the center of the pixel of the considered DEM grid.

For each considered pixel, the first value of the displacement time series is 0.0000 because the first acquisition was considered the reference one. The data recorded on the 30 × 30-m grid are interpolated according to the IDW Inverse Distance Weighting (IDW) method with nearest neighbor searching (Maleika, 2020) to cover as much analysis area as possible, including areas where

10.3389/fbuil.2023.1129175

TABLE 5 No correlation coefficients among the parameters.

		Horizontal structure				Number of floors				Age of construction				
		R.C. slab (%)	Steel slab (%)	Timber slab (%)	Vaults (%)	1–2 (%)	3–4 (%)	5–6 (%)	7+ (%)	Before 1900 (%)	1901–1943 (%)	1944–1962 (%)	1963–1971 (%)	After 1971 (%)
Horizontal structure	R.C. slab	0				55	55	92	100	99	97	67	64	77
	Steel slab		0			42	61	97	100	86	69	78	92	92
	Timber slab			0		52	51	96	100	62	75	100	99	98
	Vaults				0	27	76	100	100	47	84	93	100	98
Number of floors	1–2	50	66	92	100	0				90	88	77	81	78
	3–4	41	73	91	100		0			90	85	72	76	90
	5–6	23	84	95	100			0		94	88	75	53	95
	7+	62	85	100	100				0	92	92	69	92	100
Age of construction	Before 1900	97	59	68	77	49	55	97	100	0				
	1901–1943	88	32	85	95	53	53	95	100		0			
	1944–1962	28	75	100	99	55	52	94	99			0		
	1963–1971	11	90	100	100	58	55	88	100				0	
	After 1971	17	85	99	100	30	73	98	100					0

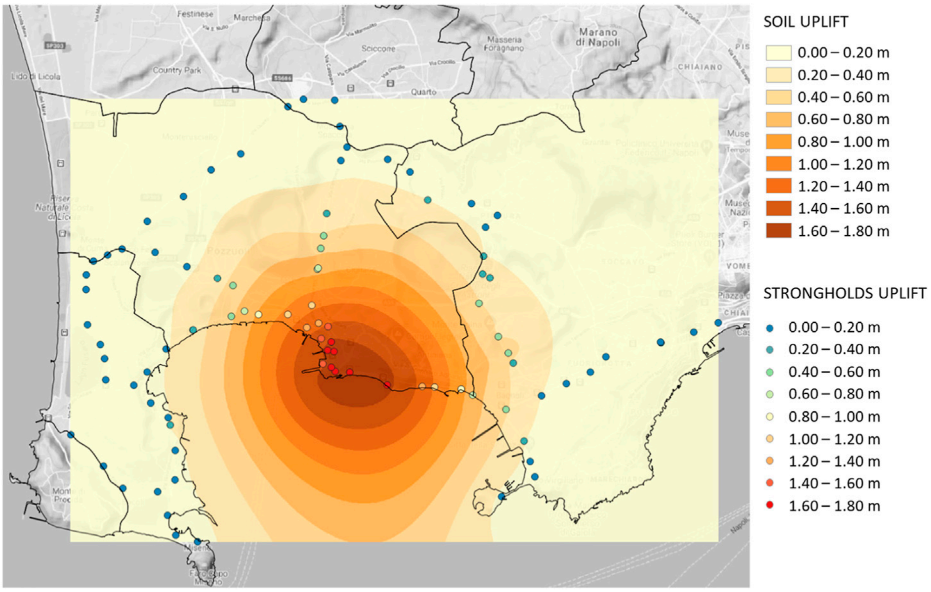

FIGURE 4
Map of the maximum vertical ground movements occurring in the 1982–1984 bradyseismic crisis, obtained through the b-spline function.

there are no SAR data (e.g., waters and vegetated areas). The obtained values are analyzed according to the 250 × 250-m analysis grid by attributing the relevant calculated statistical values to each element. The uplift of the cell has been calculated as the average of the uplifts associated with the CNR-IREA points belonging to the cell. The slope assigned to the cell is defined as the average of the slopes among the CNR-IREA points belonging to the cell, estimated based on the uplifts. Figures 8,9 show the maps of the uplifts and slopes, respectively, with reference to the detection dated 15 December 2022, where the hazard values characterizing the investigated area are minimum uplift 0.00 m, medium uplift 0.42 m, maximum uplift 1.75 m, minimum slope 0.00%, medium slope 0.012%, and maximum slope 0.030%.

3.3 Exposure and vulnerability models

Vulnerability and exposure represent strictly connected factors. For each category of exposed elements, the assessment of vulnerability due to a given natural event must be combined with "a qualitative and quantitative analysis of the exposed element" (exposure) to identify the time-spatial distribution of typological classes of exposed elements, defined as "vulnerability classes." Each represents a group of elements with the same characteristics, which presents a similar behavior (vulnerability) with respect to a given phenomenon.

In this procedure, the adopted vulnerability model is constituted by the empirical fragility curves developed in Section 2.3. In order to link these curves with the exposure, the distribution on the territory of the typological–structural characteristics of the buildings has been expressed in terms of "vulnerability classes" distribution, assessed according to the procedure developed in Section 2.2 for each cell of 250 × 250 m.

Based on the data collected using the POZZUOLI form, a correlation between the construction age of the (about 2,000) surveyed buildings and the vulnerability classes has been defined. The ISTAT 2011 (ISTAT, 2001) database furnishes, for census areas, the number of buildings for the age of construction for the following classes: before 1919, 1919–1945, 1946–1961, 1962–1971, 1972–1981, 1982–1991, 1991–1996, 1997–2001, and 2001–2011. Given the percentage of buildings associated with each vulnerability class (Table 9) (Cacace et al., 2018), using relation (Eq. 6), it is possible to identify the number of buildings associated with each vulnerability class in the census area (Table 9):

$$E_j^k = \sum_i E_{ij} \cdot p_i^k \tag{6}$$

where E_j^k is the number of buildings in the census area j with vulnerability class k; E_{ij} is the number of buildings in the census area j with the age of construction i; and p_i^k is the percentage of buildings with class k associated with the age of construction i calculated with the same procedure presented in (Cacace et al., 2018) but referred to the bradyseismic data (Table 9).

The number of buildings for each cell c belonging to the vulnerability class k is computed as follows:

$$E_c^k = \sum_{i=1}^{n} E_{ij}^k \tag{7}$$

where $E_{ij}{}^k$, the number of buildings in zone i of the census area j belonging to the vulnerability class k, is

$$E_{ij}^k = \begin{cases} E_{ij}^{k,R} & \text{when: } E_j^{census} \big/ E_j^R \leq 1 \\ E_{ij}^{k,R} + E_{ij}^{k,R} = E_{ij}^{k,R} + E_j^k \big/ E_j^{census} \cdot \left(E_{ij} - E_{ij}^R\right) & \text{when: } E_j^{census} \big/ E_j^R > 1 \end{cases} \tag{8}$$

TABLE 6 Surveyed building distribution on the levels of damage according to the uplift and slope parameters.

Class	Uplift (m)	D0	D1	D2	D3	D4	D5	Slope (-)	D0	D1	D2	D3	D4	D5
A	0.20	0	14	37	18	3	0	0.002	0	7	22	58	14	0
	0.40	0	6	34	28	4	0	0.006	0	6	15	26	6	0
	0.60	0	7	41	56	12	0	0.010	0	9	28	52	16	0
	0.80	5	8	21	31	9	0	0.014	1	13	43	104	18	0
	1.00	0	4	16	28	13	0	0.018	0	10	42	74	26	0
	1.20	0	5	20	19	5	0	0.024	2	17	82	92	18	0
	1.40	1	19	80	131	31	0	0.028	3	14	63	90	28	0
	1.60	1	20	67	219	65	0	0.030	1	7	21	34	16	0
B	0.20	6	30	57	12	0	0	0.002	0	8	28	11	1	0
	0.40	3	38	49	25	2	0	0.006	0	1	6	7	0	0
	0.60	9	37	51	22	0	0	0.010	3	13	34	21	1	0
	0.80	7	35	36	16	1	0	0.014	9	30	43	19	1	0
	1.00	1	14	32	9	0	0	0.018	4	45	56	21	0	0
	1.20	1	12	22	8	0	0	0.024	8	29	62	33	2	0
	1.40	4	25	55	37	0	0	0.028	8	67	101	47	1	0
	1.60	5	18	46	37	3	0	0.030	4	16	18	7	0	0
C	0.20	2	45	10	2	0	0	0.002	1	18	7	1	0	0
	0.40	3	43	17	8	1	0	0.006	0	11	1	1	0	0
	0.60	1	93	34	2	0	0	0.010	2	41	16	3	0	0
	0.80	6	77	28	1	0	0	0.014	1	55	10	3	0	0
	1.00	2	30	35	1	0	0	0.018	3	39	12	4	0	0
	1.20	2	67	19	0	0	0	0.024	6	120	34	9	3	0
	1.40	4	99	39	7	2	0	0.028	6	206	112	4	0	0
	1.60	3	68	21	4	0	0	0.030	4	32	11	0	0	0

c is the cell, j the census area, i the zone, that is, the intersection of the cell with the census area (Figure 10), k the vulnerability class (k = A, B, C), n the number of zones in the cell c, E_j^{census} the number of buildings in the census area j, E_j^k the number of buildings in the census area j belonging to the vulnerability class k, E_j^R the number of surveyed buildings in the census area j, $E_{ij}^{k,R}$ the number of surveyed buildings in zone i of the census area j belonging to the vulnerability class k, and $E_{ij}^{k,R}$ the number of not surveyed buildings in zone i of the census area j belonging to the vulnerability class k.

The number of buildings for each cell belonging to vulnerability Classes A, B, and C, respectively, and their percentages are reported in Figures 11, 12, 13. Over the 6,658 buildings placed in the investigated area, the model provides 17% belonging to vulnerability Class A, 37% to Class B, and 46% to Class C.

3.4 Outputs

Finally, the number of buildings of cell i reaching the damage level k caused by the hazard level j (associated with the cell) equals

$$E_{ij}^{Dk} = \sum_{l} E_{l,i} \cdot P_{l,j}^{Dk} \tag{9}$$

where $E_{l,i}$ are the buildings belonging to class l in cell i and $P_{l,j}^{Dk}$ is the probability to have a level of damage k for the vulnerability class l under the effect of hazard j, computed by the vulnerability curves (Figures 6, 7).

Figures 14, 15 show, for each cell, the percentage of buildings affected by a given level of damage depending on the hazard values (uplift and slope, respectively) provided by CNR-IREA on 15 December 2022. The impact model evaluates light damage to load-bearing structures (D2–D5) and light damage to nonstructural elements (D1).

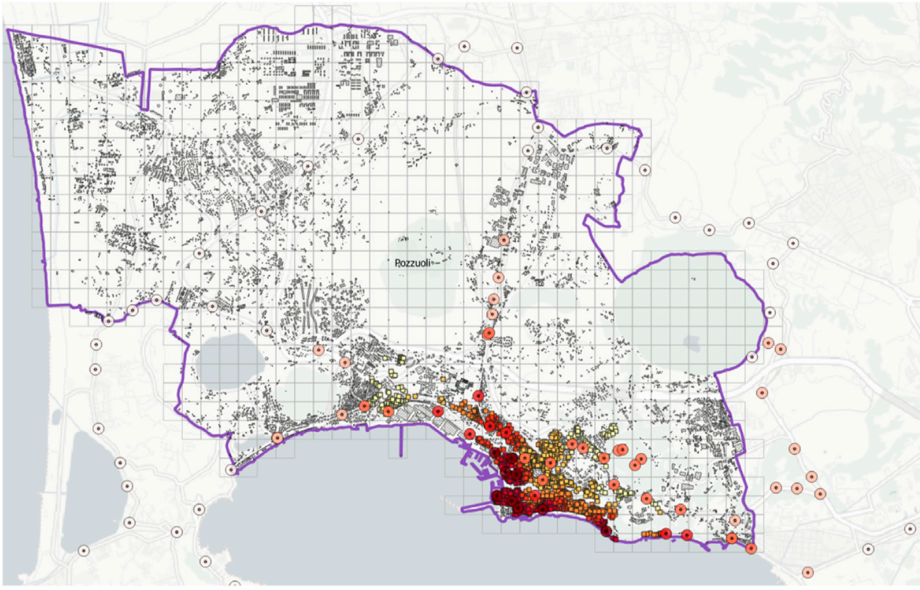

FIGURE 5
Location of the strongholds of the INGV stations and the buildings surveyed using the POZZUOLI form.

TABLE 7 Total building distribution on the levels of damage according to the uplift and slope parameters.

Uplift (m)	Class A buildings	Class B buildings	Class C buildings	Slope (-)	Class A buildings	Class B buildings	Class C buildings
0.20	532	797	1,003	0.002	281	452	563
0.40	98	146	172	0.006	246	248	304
0.60	151	190	214	0.010	117	150	179
0.80	152	203	251	0.014	186	162	164
1.00	109	89	99	0.018	157	123	137
1.20	147	124	140	0.024	300	293	331
1.40	281	163	180	0.028	425	418	486
1.60	381	180	152	0.030	84	47	48

4 Discussion, conclusion, and future developments

Campi Flegrei active caldera is a very densely urbanized area with a consequent very high volcanic risk. The occurrence of several bradyseism episodes characterized by ground uplift and subsidence according to a bell-shaped geometry centered in Pozzuoli town caused damage to the buildings and, consequently, to the resident population. During the last bradyseismic episode, which occurred in 1982–1984, the Secretary of State Minister for Coordination of Civil Protection appointed a TSC for Bradyseism in the Campi Flegrei area that, among the various carried out activities, built up the POZZUOLI form to define the state of the constructions and, in particular, the capacity of buildings for future response. The damage caused by the 1982–1984 bradyseismic event was documented in a sample of about 3,700 buildings.

In recent years, at Campi Flegrei caldera, a new phase started with increasing uplift rates over time. This phenomenon has drawn the attention of the Civil Protection Department (DPC), which is responsible for emergency coordination and relief activities. Therefore, under the VIRA agreement (VIRA 2019–2022, "Assessments of Vulnerability, Impact and Risk Induced by Campania Volcanoes on the Urban Environment") signed between DPC and the PLINIVS Study Centre, one of the DPC competence centers, a near real-time impact study of the bradyseismic phenomenon on the built environment was conducted. Based on this agreement, the PLINIVS Study Centre produced a web application for the Civil Protection Department

10.3389/fbuil.2023.1129175

TABLE 8 Surveyed building distribution on the levels of damage according to the uplift and slope parameters.

Class	Uplift (m)	D0	D1	D2	D3	D4	D5	Slope (-)	D0	D1	D2	D3	D4	D5
A	0.20	460	14	37	18	3	0	0.002	180	7	22	58	14	0
	0.40	26	6	34	28	4	0	0.006	193	6	15	26	6	0
	0.60	35	7	41	56	12	0	0.010	12	9	28	52	16	0
	0.80	83	8	21	31	9	0	0.014	8	13	43	104	18	0
	1.00	48	4	16	28	13	0	0.018	5	10	42	74	26	0
	1.20	98	5	20	19	5	0	0.024	91	17	82	92	18	0
	1.40	20	19	80	131	31	0	0.028	230	14	63	90	28	0
	1.60	10	20	67	219	65	0	0.030	6	7	21	34	16	0
B	0.20	698	30	57	12	0	0	0.002	404	8	28	11	1	0
	0.40	32	38	49	25	2	0	0.006	234	1	6	7	0	0
	0.60	80	37	51	22	0	0	0.010	81	13	34	21	1	0
	0.80	115	35	36	16	1	0	0.014	69	30	43	19	1	0
	1.00	34	14	32	9	0	0	0.018	1	45	56	21	0	0
	1.20	82	12	22	8	0	0	0.024	167	29	62	33	2	0
	1.40	46	25	55	37	0	0	0.028	202	67	101	47	1	0
	1.60	76	18	46	37	3	0	0.030	6	16	18	7	0	0
C	0.20	946	45	10	2	0	0	0.002	537	18	7	1	0	0
	0.40	103	43	17	8	1	0	0.006	291	11	1	1	0	0
	0.60	85	93	34	2	0	0	0.010	119	41	16	3	0	0
	0.80	145	77	28	1	0	0	0.014	96	55	10	3	0	0
	1.00	33	30	35	1	0	0	0.018	82	39	12	4	0	0
	1.20	54	67	19	0	0	0	0.024	165	120	34	9	3	0
	1.40	33	99	39	7	2	0	0.028	164	206	112	4	0	0
	1.60	59	68	21	4	0	0	0.030	5	32	11	0	0	0

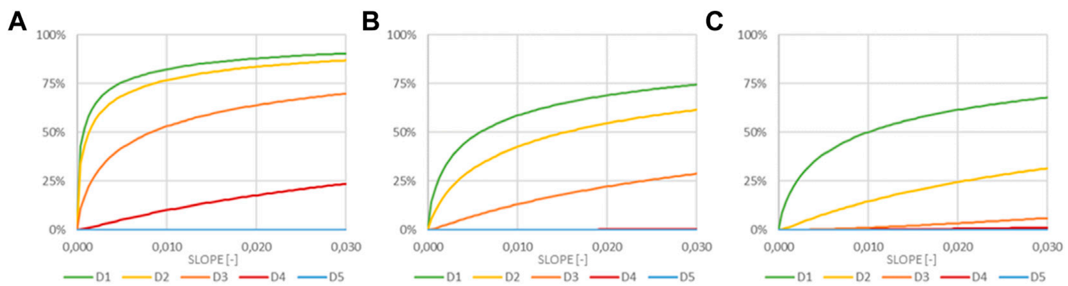

FIGURE 6
Vulnerability curves for Classed A **(A)**, B **(B)**, and **(C)** depending on slope.

based on satellite data monthly provided by CNR-IREA regarding ground uplift, giving the impact, in terms of damage, on the built-up area divided by a grid of 250 × 250 m cells. The exposure and vulnerability models adopted by the web application were obtained on an empirical basis from the survey data of the POZZUOLI forms, and the outcomes are provided for each cell in terms of building six-level damage distribution. Models used for each risk factor (hazard, exposure, and vulnerability) are described, and the impact relative to

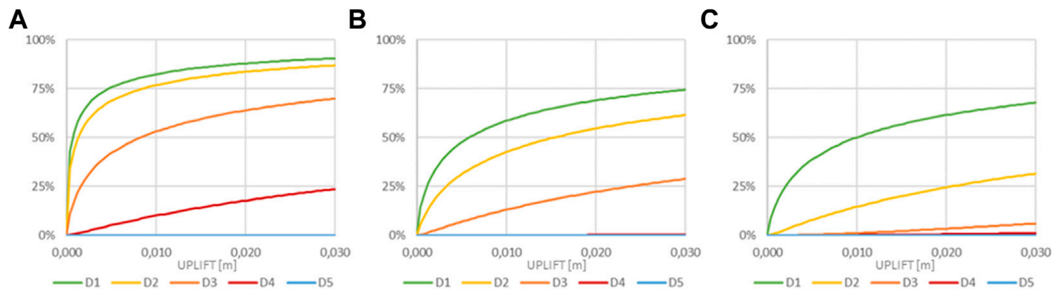

FIGURE 7
Vulnerability curves for Classed A **(A)**, B **(B),** and **(C)** depending on uplift.

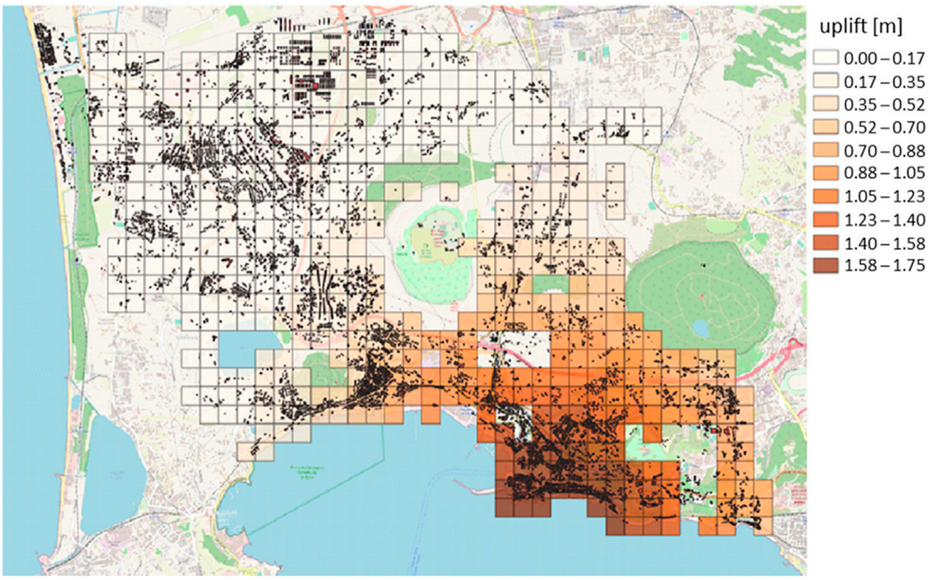

FIGURE 8
Uplift values at the cells (250 × 250 m) with reference to the detection dated 15 December 2022.

TABLE 9 Number of buildings associated with each vulnerability class on the census area.

Age of construction	Vulnerability class						Total buildings	
	Class A buildings		Class B buildings		Class C buildings			
	n°	(%)	n°	(%)	n°	(%)	n°	(%)
Before 1919	287	95	11	4	3	1	301	100
1919–1945	372	91	33	8	3	1	408	100
1946–1961	363	47	281	36	134	17	778	100
1962–1971	64	9	249	36	383	55	696	100
After 1972	7	1	198	42	270	57	475	100

the current hazard state is evaluated. The impact values obtained from the two implemented hazard parameters produce similar results, although the damage related to the slope is slightly higher.

The model developed on the basis of a web application for assessing the damage of ordinary buildings in almost real time due to bradyseism constitutes an innovative advance in the field of

10.3389/fbuil.2023.1129175

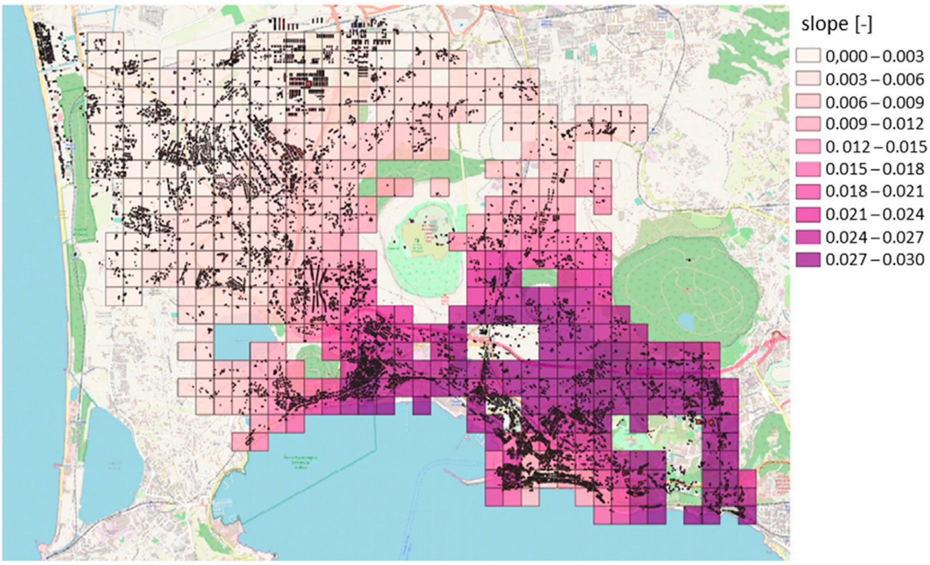

FIGURE 9
Slope values at the cells (250 × 250 m) with reference to the detection dated 15 December 2022.

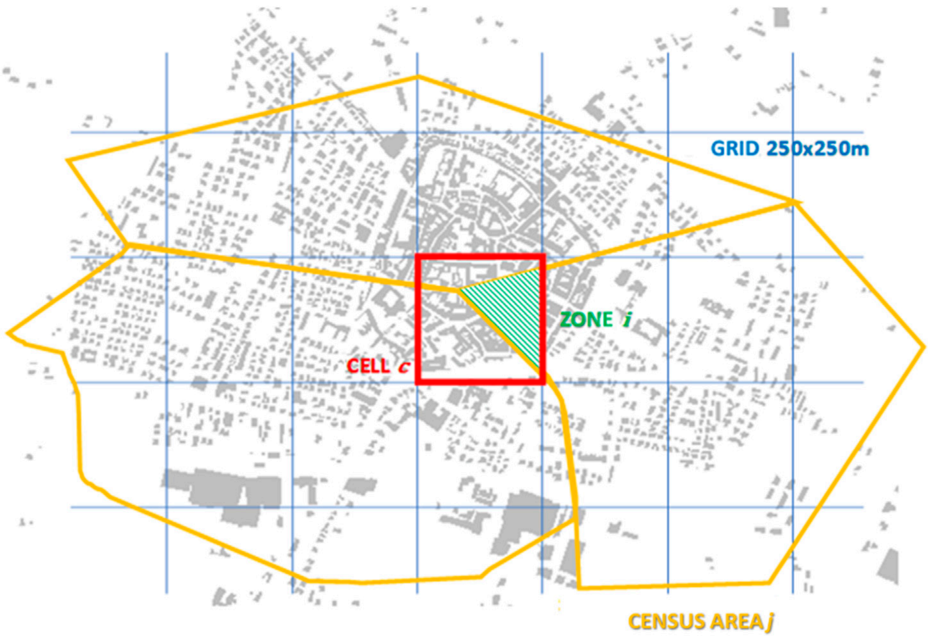

FIGURE 10
Illustrative representation of the zone (green), defined as the area of intersection between the ISTAT census area (yellow) and the 250 × 250-m cell (red) of the model reference grid (blue).

research, but it presents some critical issues. First of all, the hazard parameter adopted (uplift or slope of the center of gravity of the building plan) could be insufficient to capture some fundamental aspects of the phenomenon, such as differential settlements between the different foundation elements of the same building, as well as the speed of occurrence of the phenomenon itself. Another aspect that should not be underestimated is the development of empirical curves deduced on the basis of the observation of the damage caused by bradyseism, which occurred in 1982–1984. Such curves could be strongly influenced by the characteristics of the specific event, characterized by a given velocity (in terms of daily uplift), so extending those results to current bradyseism (which is slower)

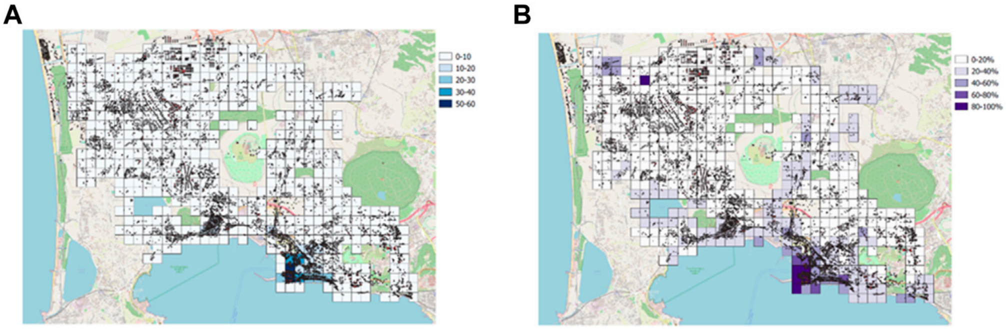

FIGURE 11
(A) Number of buildings belonging to vulnerability Class A for each cell and **(B)** their percentage.

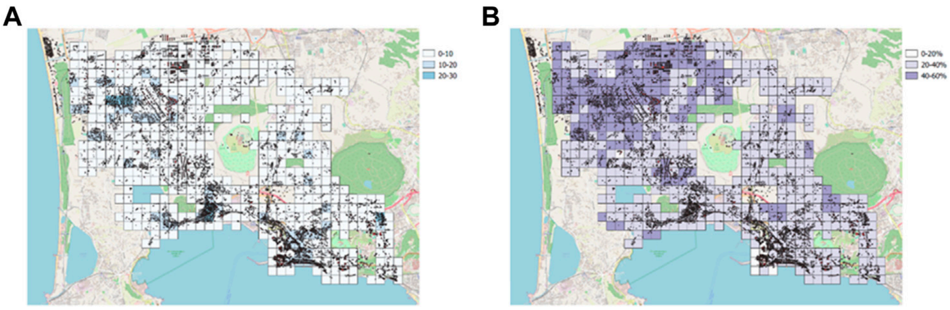

FIGURE 12
(A) Number of buildings belonging to vulnerability Class B for each cell and **(B)** their percentage.

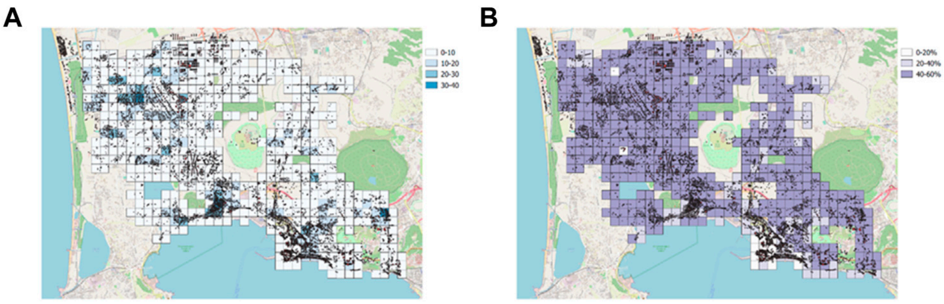

FIGURE 13
(A) Number of buildings belonging to vulnerability Class C for each cell and **(B)** their percentage.

could be overly conservative, as the presented analyses show, which estimate greater damage than those actually recorded by the Civil Protection of the Municipality of Pozzuoli. Finally, special attention should be paid to the lower damage levels (<D3), which require greater analytical attention than that possible through the POZZUOLI form, which does not capture any disturbances, such as difficulty in opening the doors and loss of verticality of the items.

Some model improvements were considered as future activities. With reference to the hazard parameters, activities are planned to install deformation sensors on some sentinel buildings that can provide punctual ground deformation values more accurately than satellite data. Further analyses are programmed to evaluate how the speed of the phenomenon affects the damage evolution. In terms of exposure, data collection activities are planned that can provide more accurate information on the vulnerability distribution over the analyzed area. Finally, it is proposed to validate the empirical vulnerability model by comparison with curves built using analytical models (Perelli et al., 2023a).

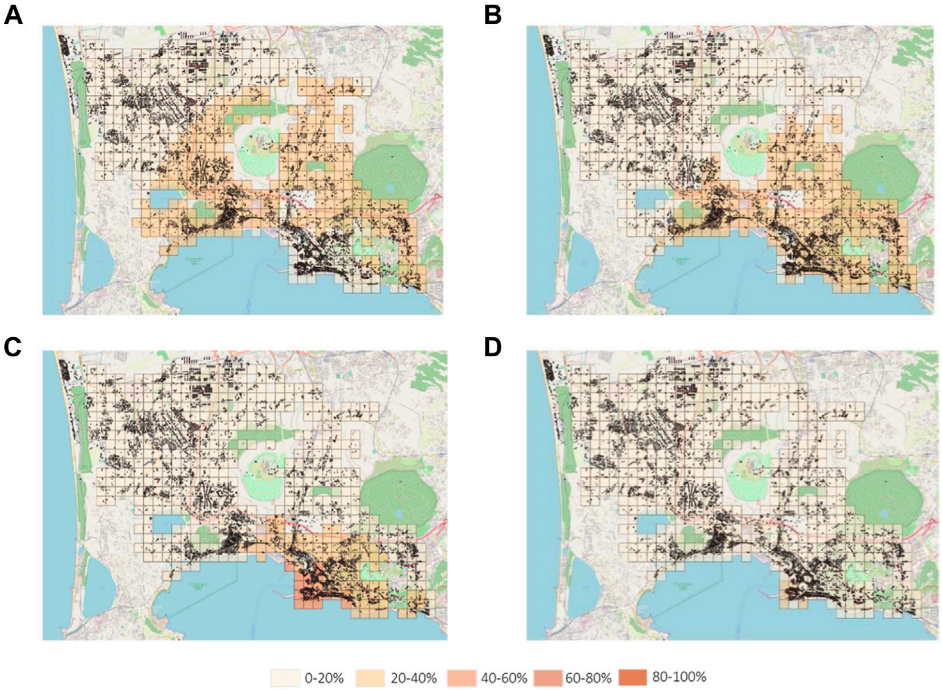

FIGURE 14
Percentage of buildings affected by damage levels D1 **(A)**, D2 **(B)**, D3 **(C)**, and D4 **(D)** with reference to the uplift reported in Figure 8.

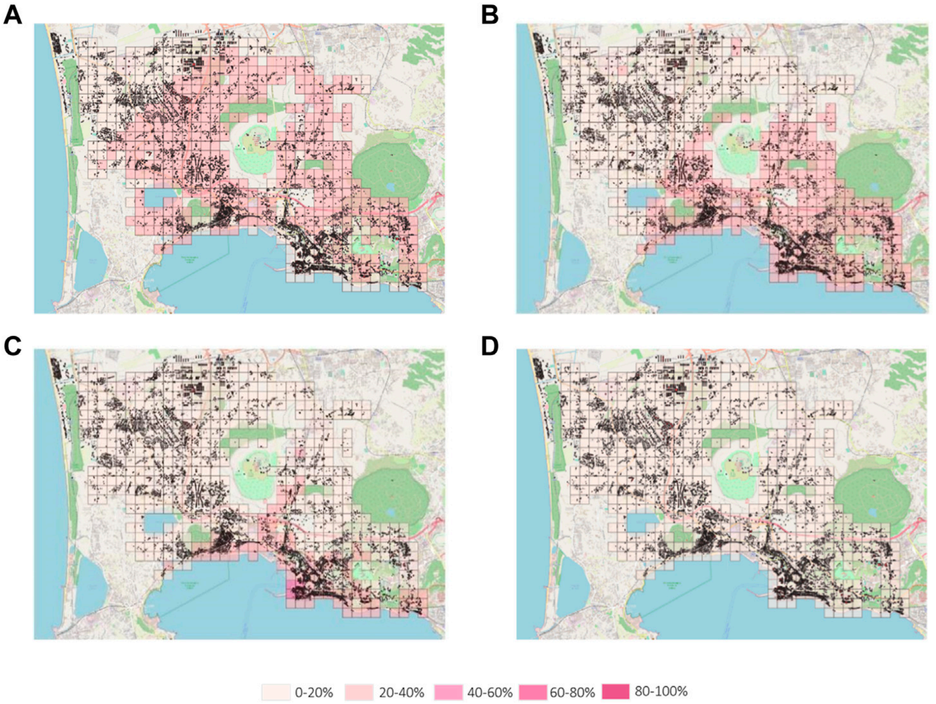

FIGURE 15
Percentage of buildings affected by damage levels D1 **(A)**, D2 **(B)**, D3 **(C)**, and D4 **(D)** with reference to the slope reported in Figure 9.

Data availability statement

The original contributions presented in the study are included in the article/supplementary materials, further inquiries can be directed to the corresponding author.

Author contributions

FP: writing–review and editing, software, formal analysis, investigation, and data curation; LD: writing–original draft, writing–review, and editing; DD: writing–original draft, writing–review and editing, conceptualization, investigation, validation, and funding acquisition; GM: review and editing; PD: review and editing; GZ: review and editing, investigation, validation, and supervision. All authors contributed to the article and approved the submitted version.

Funding

This research was developed in the framework of the VIRA 2019–2022 research project "Assessment of Vulnerability, Impact and Risk Induced by Campania Volcanoes on the Urban Environment," funded by the Italian Civil Protection Department. The described procedure is based on the activity of the Advanced Telecommunications and Information Technology Platforms for the Offer of Services to the Environmental Sector (PETIT-OSA) research project (PON 2000–2006).

Conflict of interest

The authors declare that the research was conducted in the absence of any commercial or financial relationships that could be construed as a potential conflict of interest.

Publisher's note

All claims expressed in this article are solely those of the authors and do not necessarily represent those of their affiliated organizations or those of the publisher, the editors, and the reviewers. Any product that may be evaluated in this article, or claim that may be made by its manufacturer, is not guaranteed or endorsed by the publisher.

References

Aucelli, P., Brancaccio, L., and Cinque, A. (2017). "Vesuvius and campi flegrei: Volcanic history, landforms and impact on settlements," in *Landscapes and landforms of Italy* (Springer), 389–398.

Cacace, F., Zuccaro, G., De Gregorio, D., and Perelli, F. L. (2018). Building inventory at national scale by evaluation of seismic vulnerability classes distribution based on census data analysis: BINC procedure. *Int. J. Disaster Risk Reduct.* 28, 384–393. doi:10.1016/j.ijdrr.2018.03.016

Calvi, G., Pinho, R., Magenes, G., Bommer, J., Restrepo-Vélez, L., and Crowley, H. (2006). Development of seismic vulnerability assessment methodologies over the past 30 years. *ISET J. Earthq. Technol.* 43 (3), 75–104.

Cannatelli, C., Spera, F., Bodnar, R., Lima, A., and De Vivo, B. (2020). "Ground movement (bradyseism) in the campi flegrei volcanic area: A review," in *Vesuvius, Campi Flegrei, and campanian volcanism*, 407–433.

Columbro, C., Eudave, R., Ferreira, T., Lourenço, P., and Fabbrocino, G. (2022). On the use of web mapping Platforms to support the seismic vulnerability assessment of old urban areas. *Remote Sens.* 14 (6), 1424. doi:10.3390/rs14061424

Cusano, C., Angjeliu, G., Montanino, A., Zuccaro, G., and Cennamo, C. (2021). Considerations about the static response of masonry domes: A comparison between limit analysis and finite element method. *Int. J. Mason. Res. Innovation* 6 (4), 502–528. doi:10.1504/ijmri.2021.118835

De Martino, P., Dolce, M., Brandi, G., Scarpato, G., and Tammaro, U. (2021). The ground deformation history of the neapolitan volcanic area (Campi flegrei caldera, somma–vesuvius volcano, and ischia island) from 20 years of continuous gps observations (2000–2019). *Remote Sens.* 13, 2725. doi:10.3390/rs13142725

Deino, A. L., Orsi, G., de Vita, S., and Piochi, M. (2004). The age of the Neapolitan Yellow Tuff caldera-forming eruption (Campi Flegrei caldera - Italy) assessed by 40Ar/39Ar dating method. *J. Volcanol. Geotherm. Res.* 133, 157–170. doi:10.1016/s0377-0273(03)00396-2

Del Gaudio, C., Aquino, I., Ricciardi, G., Ricco, C., and Scandone, R. (2010). Unrest episodes at campi flegrei: A reconstruction of vertical ground movements during 1905-2009. *J. Volcanol. Geotherm. Res.* 195, 48–56. doi:10.1016/j.jvolgeores.2010.05.014

Di Vito, M. A., Isaia, R., Orsi, G., Southon, J., De Vita, S., D'Antonio, M., et al. (1999). Volcanism and deformation since 12,000 years at the campi flegrei caldera (Italy). *J. Volcanol. Geotherm. Res.* 91, 221–246. doi:10.1016/s0377-0273(99)00037-2

Giudicepietro, F., Chiodini, G., Avino, R., Brandi, G., Caliro, S., De Cesare, W., et al. (2021). Tracking episodes of seismicity and gas transport in campi flegrei caldera through seismic, geophysical, and geochemical measurements. *Seismol. Res. Lett.* 92, 965–975. doi:10.1785/0220200223

Grünthal, G. (1998). *European macroseismic scale*. Luxemburg.

Harrichian, E. e. a. (2021). A review on application of soft computing techniques for the rapid visual safety evaluation and damage classification of existing buildings. *J. Build. Eng.* 43, 102536. doi:10.1016/j.jobe.2021.102536

Horwell, C. J., Baxter, P. J., and Kamanyire, R. (2015). "Health impacts of volcanic eruptions," in *Global volcanic hazards and risk*, 289–294.

Iannuzzo, A., Angelillo, M., De Chiara, E., De Guglielmo, F., De Serio, F., Ribera, F., et al. (2018). Modelling the cracks produced by settlements in masonry structures. *Meccanica* 53 (7), 1857–1873. doi:10.1007/s11012-017-0721-2

Iannuzzo, A., Dell'Endice, A., Van Mele, T., and Block, P. (2021). Numerical limit analysis-based modelling of masonry structures subjected to large displacements. Computers & Structures. *Comput. Struct.* 242. doi:10.1016/j.compstruc.2020.106372

Işık, M., Işik, E., and Bulbul, M. .A. (2018). Application of iOS/Android based assessment and monitoring system for building inventory under seismic impact. *Gradevinar* 70, 1043–1056. doi:10.14256/JCE.1522.2015

Işık, M., Işik, E., and Harı̆cı̄hı̆an, E. (2021). Application of IOS/Android rapid evaluation of post-earthquake damages in masonry buildings. *Gazi Mühendislik Bilim. Derg.* 7 (1), 36–50. doi:10.30855/gmbd.2021.01.05

ISTAT (2001). *14° censimento della popolazione e delle abitazioni*.

Jenkins, S., Wilson, T., Miller, V., Miller, V., Stewart, C., Blong, R. J., et al. (2015). "Volcanic ash fall hazard and risk," in *Global volcanic hazards and risk*, 173–221.

Liguori, F. S., Fiore, S., Perelli, F. L., De Gregorio, D., Zuccaro, G., and Madeo, A. (2022). "Seismic vulnerability of masonry structures through a mechanical-based approach," in *World congress in computational mechanics and ECCOMAS congress* (Oslo.

Lima, A., Bodnar, R., De Vivo, B., Spera, F., and Belkin, H. (2021). Interpretation of recent unrest events (bradyseism) at campi flegrei, napoli (Italy): Comparison of models based on cyclical hydrothermal events versus shallow magmatic intrusive events. *Geofluids* 2021, 1–16. doi:10.1155/2021/2000255

Maia Avelino, R., Iannuzzo, A., Van Mele, T., and Block, P. (2022). An energy-based strategy to find admissible thrust networks compatible with foundation settlements in masonry structures. *Mech. Res. Commun.* 125, 103978. doi:10.1016/j.mechrescom.2022.103978

Maleika, W. (2020). Inverse distance weighting method optimization in the process of digital terrain model creation based on data collected from a multibeam echosounder. *Appl. Geomatics* 12 (6), 397–407. doi:10.1007/s12518-020-00307-6

Marzocchi, W., Selva, J., Costa, A., Sandri, L., Tonini, R., and Macedonio, G. (2015). "Tephra fall hazard for the Neapolitan area," in *Global volcanic hazards and risk*, 239–248.

Montanino, A., De Gregorio, D., Olivieri, C., and Iannuzzo, A. (2022). The continuous airy-based for stress-singularities (CASS) method: An energy-based numerical formulation for unilateral materials. *Int. J. Solids Struct.* 256, 111954. doi:10.1016/j.ijsolstr.2022.111954

Nanda, R., Damarla, R., and Nayak, K. (2022). Android application of rapid visual screening for buildings in indian context. *Structures* 46, 1823–1836. doi:10.1016/j.istruc.2022.10.140

Orsi, G., De Vita, S., and Di Vito, M. (1996). The restless, resurgent Campi Flegrei nested caldera (Italy): Constraints on its evolution and configuration. *J. Volcanol. Geotermal Res.* 74, 179–214. doi:10.1016/s0377-0273(96)00063-7

Orsi, G., Civetta, L., Del Gaudio, C., de Vita, S., Di Vito, M. A., Isaia, R., et al. (1999). Short-term ground deformations and seismicity in the resurgent campi flegrei caldera (Italy): An example of active block-resurgence in a densely populated area. *Volcanol. Geotherm. Res.* 91, 415–451. doi:10.1016/s0377-0273(99)00050-5

Perelli, F. L., De Gregorio, D., Cacace, F., and Zuccaro, G. (2019). Empirical vulnerability curves for Italian masonry buildings. Proceeding of the 7°ECCOMAS Thematic Conference on Computational Methods in Structural Dynamics and Earthquake Engineering [COMPDYN]. Heraklion: Crete.

Perelli, F. L., De Gregorio, D., Montanino, A., Olivieri, C., Maddaloni, G., and Iannuzzo, A. (2023a). Energy-based modelling of in-plane fragility curves for the 2D ultimate capacity of Italian masonry buildings. *Front. Built Environ.* 9, 1127523. doi:10.3389/fbuil.2023.1127523

Perelli, F., De Gregorio, D., and Zuccaro, G. (2023b). *Analysis of ordinary buildings on the island of ischia (Italy) for a seismic impact*. Sidney: SSRN.

Tramelli, A., Del Pezzo, E., Bianco, F., and Boschi, E. (2006). 3D scattering image of the Campi Flegrei caldera (Southern Italy). *Phys. Earth Planet. Interiors* 155, 269–280. doi:10.1016/j.pepi.2005.12.009

Vitale, S., Isaia, R., Ciarcia, S., Di Giuseppe, M., Iannuzzi, E., Prinzi, E., et al. (2019). Seismically induced soft-sediment deformation phenomena during the volcano-tectonic activity of Campi Flegrei caldera (southern Italy) in the last 15 kyr. *Tectonics* 38 (6), 1999–2018. doi:10.1029/2018tc005267

Zhang, S., Liu, Y., and Li, S. (2022). A brief method for rapid seismic damage prediction of buildings based on structural strength. *Buildings* 12 (6), 783. doi:10.3390/buildings12060783

Zuccaro, G., and Cacace, F. (2015). Seismic vulnerability assessment based on typological characteristics. First level procedure SAVE. *Soil Dyn. Earthq. Eng.* 69, 262–269. doi:10.1016/j.soildyn.2014.11.003

Zuccaro, G., De Gregorio, D., Leone, M. F., Sessa, S., Nardone, S., and Perelli, F. L. (2021). Caesar ii tool: Complementary analyses for emergency planning based on seismic risks impact evaluations. *Sustainability* 13, 9838. doi:10.3390/su13179838

Zuccaro, G., Perelli, F. L., De Gregorio, D., and Masi, D. (2021). Caesar II: An Italian decision support tool for the seismic risk. The case study of Torre Pellice, Villar Pellice and Pinerolo municipalities. Proceeding of the 8th International Conference on Computational Methods in Structural Dynamics and Earthquake Engineering, COMPDYN 2021. Athens.